Data in Brief 53 (2024) 110096

Contents lists available at ScienceDirect

Data in Brief

journal homepage: www.elsevier.com/locate/dib

Data Article

Transesterification of *Jatropha curcas* oil to biodiesel using highly porous sulfonated biochar catalyst: Optimization and characterization dataset

Supongsenla Ao[a], Shiva prasad Gouda[a], Manickam Selvaraj[b], Rajender Boddula[c,*], Noora Al-Qahtani[c,d,**], Sakar Mohan[e], Samuel Lalthazuala Rokhum[a,*]

[a] *Department of Chemistry, National Institute of Technology Silchar, Assam 788010, India*
[b] *Department of Chemistry, Faculty of Science, King Khalid University, Abha 61413, Saudi Arabia*
[c] *Center for Advanced Materials (CAM), Qatar University, Doha 2713, Qatar*
[d] *Central Laboratories Unit (CLU), Qatar University, Doha 2713, Qatar*
[e] *Centre for Nano and Material Sciences, Jain (Deemed to be University), Jain Global Campus, Kanakapura, Bangalore, Karnataka 562112, India*

ARTICLE INFO

Article history:
Received 20 December 2023
Revised 18 January 2024
Accepted 18 January 2024
Available online 26 January 2024

Dataset link: Transesterification of Jatropha curcas oil using highly porous sulfonated biochar catalyst: Optimization and characterization dataset (Original data)

Keywords:
4-diazoniobenzenesulfonate
Jatropha curcas oil
Biodiesel
Response surface methodology

ABSTRACT

The study involves a collection of data from the published article titled "Active sites engineered biomass-carbon as a catalyst for biodiesel production: Process optimization using RSM and life cycle assessment "*Energy Conversion Management*" journal. Here, the activated biochar was functionalized using 4-diazoniobenzenesulfonate to obtain sulfonic acid functionalized activated biochar. The catalyst was comprehensively characterized using XRD, FTIR, TGA, NH_3-TPD, SEM-EDS, TEM, BET, and XPS analysis. Further, the obtained catalyst was applied for the transesterification of *Jatropha curcas* oil (JCO) to produce biodiesel. An experimental matrix was conducted using the RSM-CCD approach and the resulting data were analyzed using multiple regressions to fit a quadratic equation, where the maximum biodiesel yield

DOI of original article: 10.1016/j.enconman.2023.117956
* Corresponding authors.
** Corresponding author at: Center for Advanced Materials (CAM), Qatar University, Doha 2713, Qatar.
E-mail addresses: research.raaj@gmail.com (R. Boddula), noora.alqahtani@qu.edu.qa (N. Al-Qahtani), rokhum@che.nits.ac.in (S.L. Rokhum).

https://doi.org/10.1016/j.dib.2024.110096

achieved was 97.1 ± 0.4%, under specific reaction conditions: a reaction time of 50.3 min, a molar ratio of 22.9:1, a reaction temperature of 96.2 °C, and a catalyst loading of 7.7 wt.%. The obtained product biodiesel was analyzed using NMR and GC-MS analyzed and is reported in the above-mentioned article.

Specification Table

Subject	Energy
Specific subject area	Renewable energy, sustainability and environment
Type of data	Table Graph Figure
Data format	Raw and analyzed
Data collection	Raw data related to the production of biodiesel using GZF-SO_3H catalyst are collected. The catalyst was synthesized in a laboratory scale and applied for the production of biodiesel using *Jatropha curcas* oil feedstock. The raw data are processed using licensed software. Origin pro 2023 software was used for XRD, FTIR, TGA, BET and NH_3-TPD plot. Casa XPS 2023 software for XPS analysis result. MestReNova software for NMR prediction and OpenChrom for GC-MS result. Statistical tool Design Expert was used for RSM optimization process.
Data source location	Catalyst and biodiesel synthesis was within the chemistry laboratory, National Institute of Technology Silchar.
Data accessibility	1) All data is available within this article. 2) Repository name: Mendeley data 3) https://data.mendeley.com/datasets/3cpkgkk2tn/1 DOI:10.17632/3cpkgkk2tn.1
Related research article	This dataset is part of the result reported in "Active sites engineered biomass-carbon as a catalyst for biodiesel production: Process optimization using RSM and life cycle assessment "which was published in *Energy Conversion Management*" journal. (DOI: https://doi.org/10.1016/j.enconman.2023.117956)

Abbreviation Table

BET	*Brunauer–Emmett–Teller*
FAME	*Fatty acid methyl esters*
FTIR	*Fourier transform infrared analysis*
GC-MS	*Gas chromatography- mass spectrometry*
GZF-SO_3H	*Glucose + $ZnCl_2$ + $FeCl_3$ -sulphonic acid*
TGA	*Thermogravimetric analysis*
NH_3-TPD	*Ammonia- Temperature programmed desorption*
NMR	*Nuclear magnetic resonance*
RSM-CCD	*Response surface methodology-central composite design*
SEM-EDS	*Scanning electron microscopy-energy dispersive X-ray spectroscopy*
TEM	*Transmission electron microscopy*
XPS	*X-ray photoelectron spectroscopy*
XRD	*X-ray powder diffraction*

1. Value of the Data

- This article presents a dataset that will enhance researchers' comprehension of how the yield of biodiesel production is influenced by various operating parameters.

- *Jatropha curcas* oil as feedstocks and highly porous biochar catalyst are the leading factor in this study.
- Researchers can explore the functionalization of biomass through this finding.
- Overall, the synthesis process is maintainable for the sustainability of industrial development.

2. Background

This study quantifies the production of highly efficient and porous activated biochar by simultaneous activation-graphitization *via* pyrolysis of cheap and widely available biomass precursor (glucose). Previously, the attainment of such a high surface area was limited to metal-organic framework catalysts and commercialized chemicals, highlighting their advantages. However, this recent development has made it possible to achieve comparable surface area using sulfonic acid functionalized activated biochar, which is a significant advancement. Further, the obtained catalyst was applied for the conversion of inedible *Jatropha curcas* oil (JCO) to biodiesel yield. The experimental matrix was conducted using RSM-CCD approach, and the resulting data were analyzed using multiple regressions to fit a quadratic equation. The maximum biodiesel yield achieved was 97.1 $\pm$ 0.4%, which was obtained with specific reaction conditions: a reaction time of 50.3 min, a molar ratio of 22.9:1, a reaction temperature of 96.2 °C, and a catalyst loading of 7.7 wt.%. The physico-chemical properties of the obtained biodiesel met the acceptable standards set by ASTM for standard biodiesel. The catalyst demonstrates excellent recyclability, maintaining a high yield over seven reaction cycles with minimal loss. Herein, the discovery presents a significant opportunity for large-scale commercialization by the discovery of biomass-derived activated carbon.

3. Data Description

The data provided in this paper were collected from the recent paper published titled "Active sites engineered biomass-carbon as a catalyst for biodiesel production: Process optimization using RSM and life cycle assessment" [14]. The raw data is now submitted to Mendeley data repository and can be downloaded at https://data.mendeley.com/datasets/3cpkgkk2tn/1 and has been made openly accessible. The repository consists of 9 processed raw files of the catalyst and FTIR of biodiesel in excel sheets each named accordingly and to have a better understanding of the processed data each file will be systematically explained in the following paragraph.

3.1. BET Characterization

Catalyst was degassed for 10 h at 150 °C on a Micromeritics ASAP 2010 surface area and porosity detector before being examined using the BET method. The N_2 adsorption–desorption isotherms were calculated using a Micromeritics ASAP 2010 surface area and porosity analyzer. An ESCALAB Xi + system with a micro-focused dual-anode Al/Mg K source was utilized to conduct the XPS analysis. The samples were heated to a maximum temperature of 50 °C at a rate of 5 °C/min using a flow of helium (100 cm^3/min).

Excel sheet No. 1 of the data repository contains the data of BET analysis. The result is explained here in Fig. 1. It shows the N_2 adsorption–desorption isotherm for the GZF-SO_3H catalyst. This isotherm showed a type IV hysteresis loop and isotherm, which indicates that the catalyst exhibits non-homogeneous mesoporous characteristics. According to Barrett, Joyner, and Halenda's (BJH) analysis of the pore size distribution, the range was 4.12 nm. The high catalytic surface area and pore volume, at 1196.13 m^2 g^{-1} and 0.7711 cc g^{-1}, respectively, both were within the anticipated ranges [3].

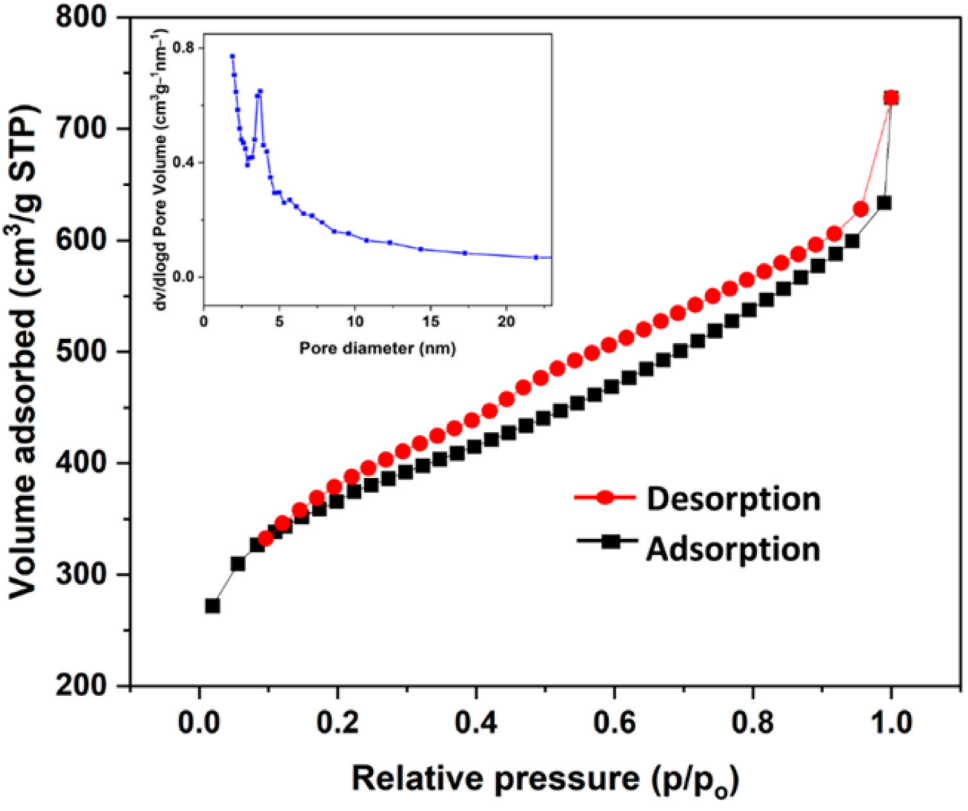

Fig. 1. N_2 adsorption-desorption isotherm and BJH pore size distribution curve (inset) of GZF-SO_3H catalyst [14].

3.2. XRD Characterization

XRD give us information about the state of compound, whether it is in the form of amorphous or crystallinity structure. Here, Fig. 2a shows the XRD characterization of GZF-SO_3H catalyst. The graph exhibits 2θ range of 20–30°, corresponding to the (002) plane of the carbonized material derived from glucose [1,2] confirming the amorphous nature of the catalyst. The file can now be accessed in Excel sheet No. 9 of the repository. The XRD investigation was performed using a PANalytical X'Pert Pro diffractometer. Cu Kα radiation was employed within the range of 2θ = 20–60°, while the operational voltage and current were set at 40 kV and 100 mA, respectively.

3.3. FTIR Characterization

Excel sheet No. 2 of the Mendeley data repository give us the processed data of FTIR analysis. FTIR analysis was done to discover the presence of functional groups in the elements. Here, FTIR analysis (Fig. 2b) revealed specific peaks associated with different functional groups. At 1106 cm^{-1}, a peak was observed, subsequent to the symmetric stretching of SO_3^-. Formation of peaks can be seen at 1365 cm^{-1} and 1591 cm^{-1}, indicating the presence of carbonyl stretching (C=O) and C=C stretching in aromatic rings, respectively [3,4]. The stretching and bending vi-

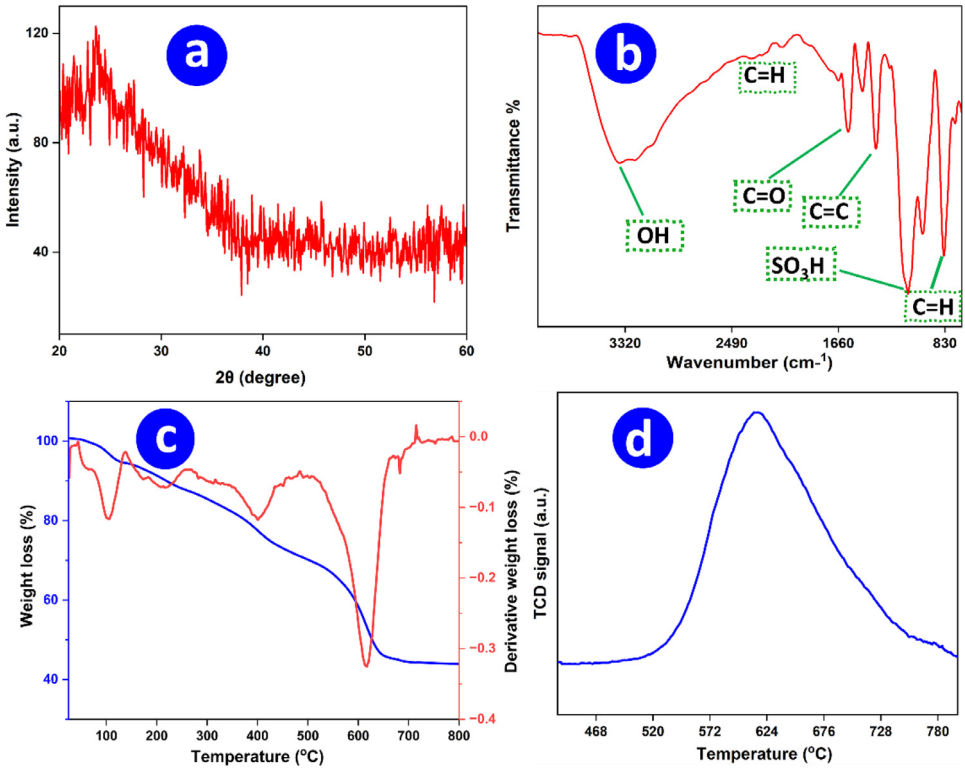

Fig. 2. XRD pattern (a), FT-IR spectrum (b), and TGA/DTG data (blue and red lines, respectively; (c) NH_3-TPD profile (d) of as-prepared GZF-SO_3H catalyst [14].

bration of C-H bonds were visible at 2482 cm^{-1} and 830 cm^{-1}. Furthermore, a broad absorption around 3120 cm^{-1} indicated the O-H stretching [5,6].

The variable used for the study was attained in the range between 400 and 4000 cm^{-1} with a 3000 Hyperion FTIR spectrometer (Bruker, Germany) at 25 °C.

3.4. TGA Characterization

Excel sheet No. 7 of the Mendeley data repository contained the processed TGA data. The obtained data (Fig. 2c) indicated a mass loss of approximately 11% between 70 and 150 °C, which was attributed primarily to the removal of adsorbed water as the catalyst tend to absorb moisture in an open environment. The catalyst decreased linearly up to 350 °C before it began to decompose developing a weight loss of 10% which was attributed to disintegration of -SO_3H on carbon surface. Further breakdown at a temperature between 550 and 675 °C corresponds to the decomposition of the organic carbon structure present in the catalyst.

Thermogravimetric analysis of the catalyst was evaluated in the temperature range of 50–800 °C TGA of the catalyst was performed using a TG/DTA (model no. STA 409 Netzsch Geratebau GMBH, Germany) under airflow at 1.5 bar and 2 L h^{-1} with the degassing temperature between 50 and 800 °C.

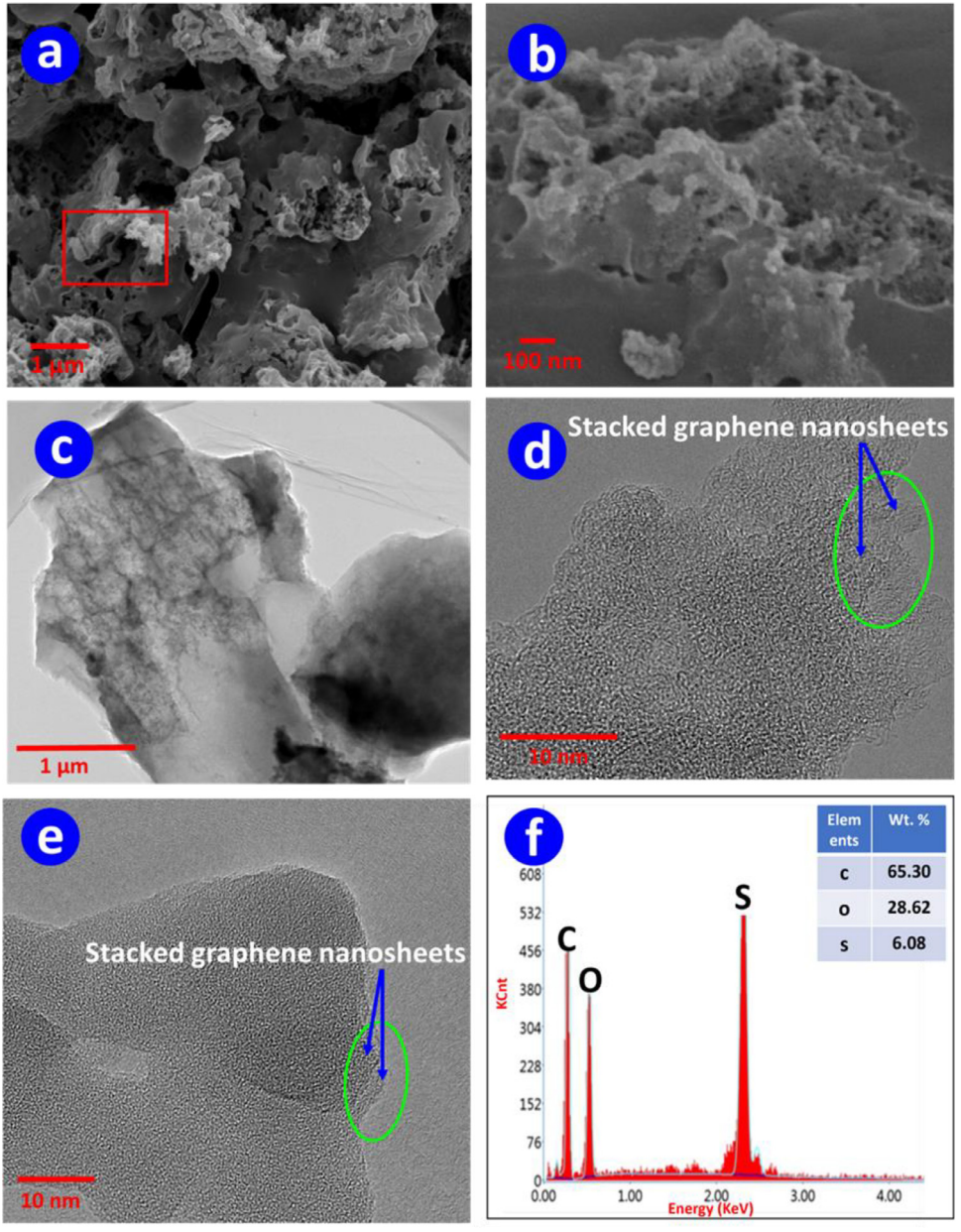

Fig. 3. Representative SEM micrographs of GZF-SO_3H catalyst. Scale bars 1 μm (a), 100 nm (b), TEM results of graphitic sheet micrograph at scale bars 1 µm (c), 10 nm (d and e) and EDS data for the red-boxed area (f) of image (a) [14].

3.5. NH_3-TPD Characterization

Excel sheet No. 5 in the repository data contains NH_3-TPD data. Temperature-programmed desorption (TPD) was exploited to determine the acidity and strength of the catalysts' surfaces using NH_3 as a probe molecule using a thermal conductivity detector (TCD)-equipped ChemiSorb

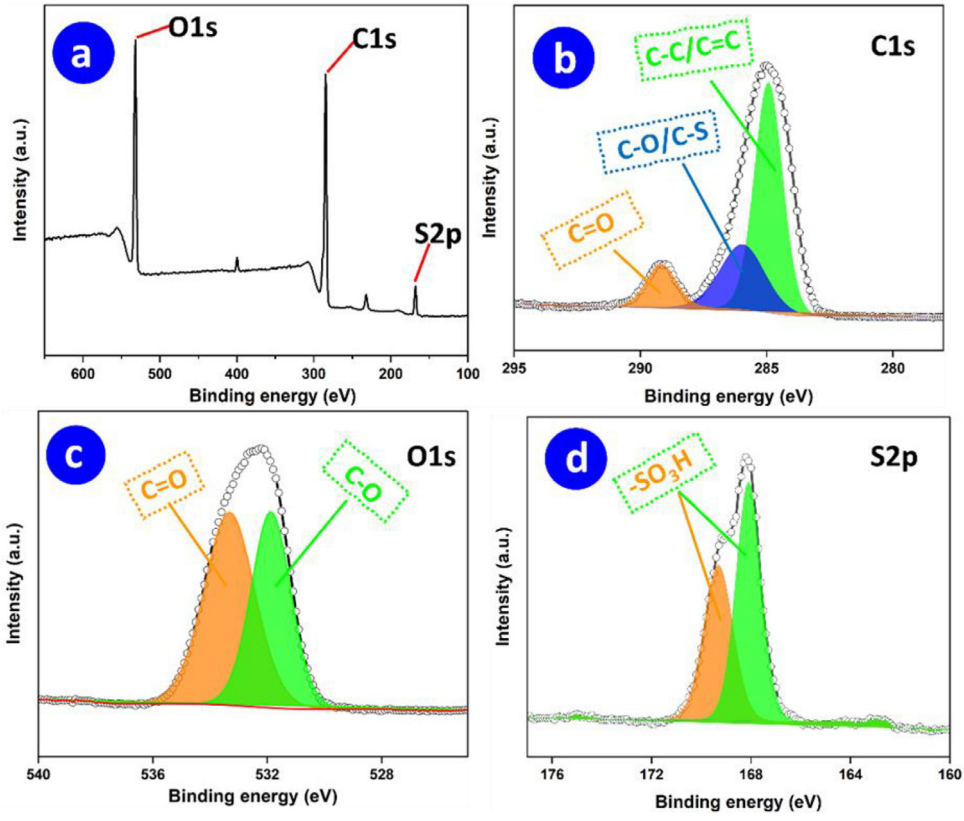

Fig. 4. Overall XPS survey spectrum (a) and deconvoluted XPS signals (blue, orange, green) as well as raw (white bubble) data for C1s (b), O1s (c), and S2p (d) regions of GZF-SO_3H catalyst [14].

2720 analyzer. To eliminate water from the catalysts, the samples underwent a pretreatment under N2 at 200 °C for 1 h.

NH_3-TPD profile of the GZF-SO_3H catalyst displayed 2.4 mmol g^{-1} of the total acid sites (Fig. 2d). A well-resolved ammonia desorption peaks at a temperature corresponding strong acid site, at 615 °C shows that the synthesized catalyst has the acid site requirements for effective protonation [7].

3.6. SEM-EDX and TEM Characterization

Using a ramping rate of 10 °C min^{-1} to 800 °C under argon, the samples were heated after being purged with N_2 and saturated with 5 mL min^{-1} of pure ammonia for 30 min at 25 °C. The size, shape, and composition of elements in the catalyst were assessed using scanning electron microscopy (SEM) and energy-dispersive X-ray spectroscopy (EDS) techniques. The SEM analysis was conducted using a JEOL JSM-7600F instrument, while the FEI Quanta 200F instrument equipped with a tungsten-doped lanthanum hexaboride (LaB6) X-ray source and an ETD detector was utilized for acquiring SEM images. The SEM imaging was performed under high vacuum conditions, utilizing secondary electrons and a 30 kV acceleration voltage. Catalyst was dissolved in ethanol and drop cast onto a Cu grid for transmission electron microscopy (TEM), which was followed by oven drying. A JEOL JEM2100 microscope was used to capture the images.

Table 1
Chemical composition of product JCO biodiesel [14].

Peak No.	Component name	Retention time (mins.)	Corresponding acid	Proportion (%)
1.	Hexadecanoic acid methyl ester	12.613	C16:0	18.956
2.	Linoleic acid methyl ester	13.744	C18:2	22.84
3.	9-Octadecenoic acid, methyl ester, (E)	13.780	C18:3	38.986
4.	Methyl stereate	13.909	C18:0	10.871
5.	Methyl 12, 13- epoxy-13-methoxy, 9 octadecenoate	14.558	C19:1	2.448
6.	Octanedioic acid, 4-isopropyl-, dimethyl ester	15.518	C11:0	3.511
7.	Octadecanoic acid, 9,10-dihydroxy-, methyl ester	15.606	C18:0	2.388

Scanning electron micrographs revealed a highly mesoporous porous carbon network structure (Fig. 3a and b) and it is made up of a variety of random arbitrary particles, whose cluster can be attributed to the carbonization process's leading to the elimination of water [8]. Meanwhile, TEM micrographs in varying resolution (Fig. 3c–e) demonstrated the complete resolution of the structure into stacked and irregularly folded porous graphene-like nanosheets confirming the high graphitized carbon [9,10]. EDS data (Fig. 3f) of the area highlighted in SEM image Fig. 3a displayed the successful sulphonation of activated carbon revealing sulfur of ~6.08 wt.% equivalent to be around 1.9 mmol g^{-1}.

3.7. XPS Characterization

An ESCALAB Xi+ system with a micro-focused dual-anode Al/Mg K source was utilised to conduct the XPS analysis shown in excel sheet No. 8 of the data repository. The samples were heated to a maximum temperature of 50 °C at a rate of 5 °C/min using a flow of helium (100 cm^3/min).

On the acidic GZF-SO_3H catalyst, XPS analysis (Fig. 4) was performed. The survey spectrum (Fig. 4a) showed that C1s, O1s, and S2p were present in the catalyst. The C1s region's deconvoluted spectra (Fig. 4b) showed strong peaks at 284.9 eV corresponding to C-C/C=C both in the aromatic and aliphatic group, while that 286.0 eV corresponds to phenolic, alcoholic, and alkoxy compound respectively, and peak at 289.2 eV, corresponds to COOH group [11,12]. The O1s spectra with two deconvoluted peaks are shown in Fig. 4c. The organic groups (i.e., aromatic rings and phenols) that are bound to C-O and C=O/S=O result in peaks at 531.8 and 533.4 eV, respectively [11]. The S2p spectrum (Fig. 4d) is deconvoluted into two peaks, S2p $_{3/2}$ at 168.0 eV and S2p $_{½}$ at 169.3 eV due to spin-orbit coupling which were ascribed to sulfur in the SO_3H groups and indicate successful sulfonation [13]. Further, the result of XPS revealed that 1.5 mmol g^{-1} of sulfur was present in the catalyst which is in line with the SEM-EDS analysis (Fig. 3).

3.8. Heterogeneity Test and Catalyst Reusability Operation

Hot Sheldon filtration method was performed to confirm the heterogeneity of the catalyst. The obtained data after performing the test is uploaded in excel sheet No. 4 of the repository. For the process, the catalyst was separated from the reaction mixture after 40 min, and 91.53 ± 1.4 yield of biodiesel was observed (Fig. S2). Subsequently, the reaction continued for another 15 min without the catalyst in it. It was stated that there was an increase in the biodiesel yield of 2.39%. The result proved that still some remnants of the catalyst are present in the reaction mixture that prompted the increase in conversion of JCO to biodiesel yield, which proved the heterogeneity of the catalyst.

To test the recyclability of the catalyst, the used catalyst was first isolated from the reaction mixture *via* centrifugation, then the catalyst was collected and washed with methanol and

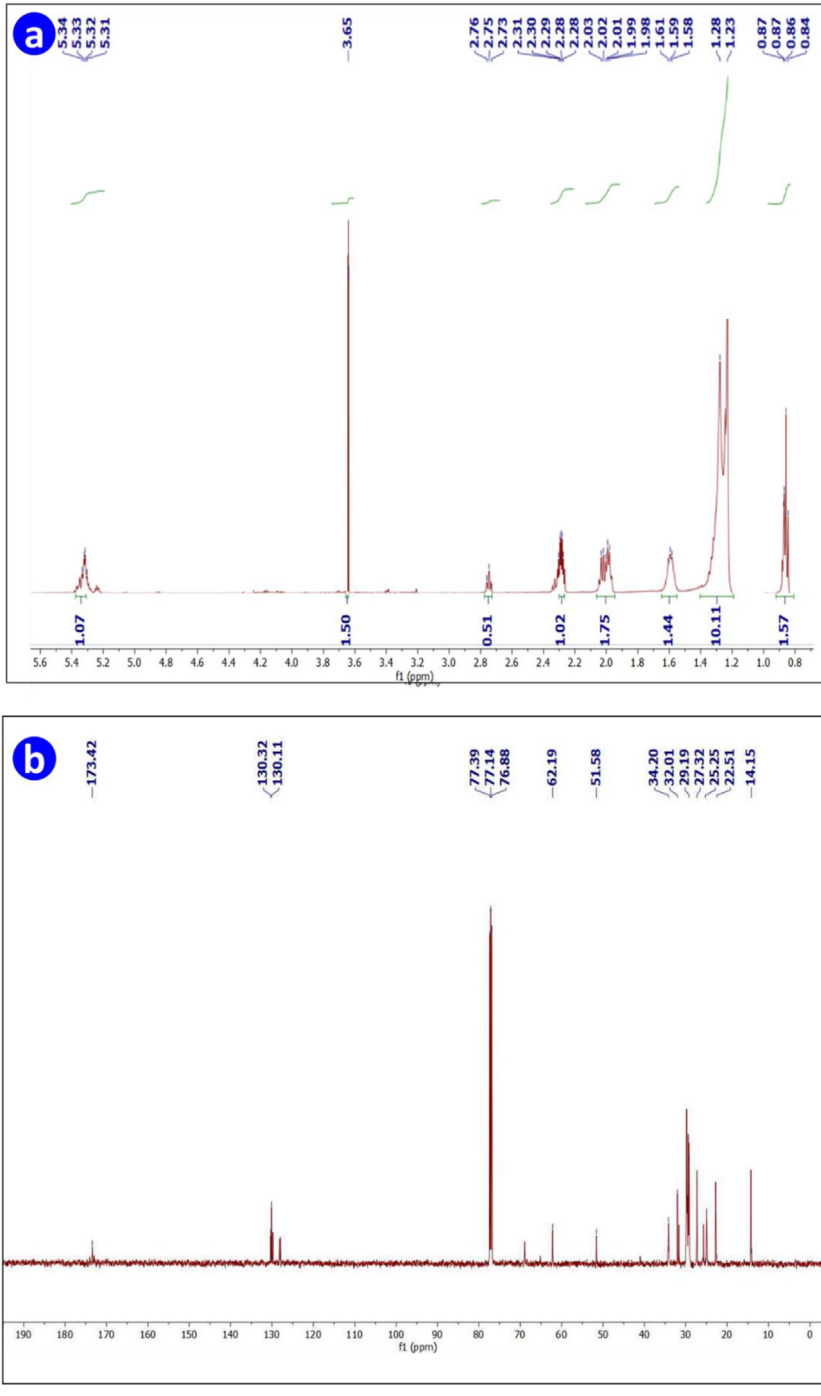

Fig. 5. ^{1}H NMR and $\{^{1}H\}^{13}C$ NMR spectra of the synthesized biodiesel from JCO [14].

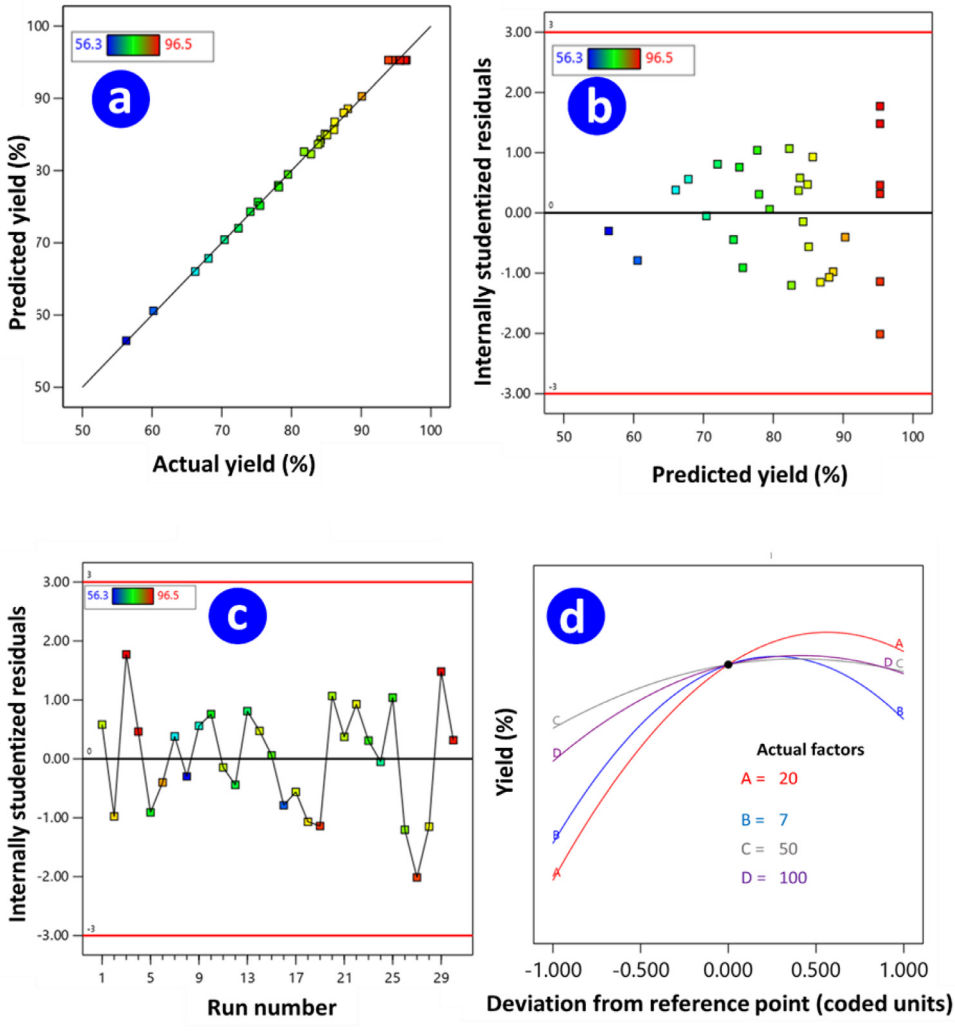

Fig. 6. Diagnostics plots of (a) Actual vs prediction of biodiesel yield (b) Studentized residual vs predicted biodiesel yield (c) residual differences between predicted and actual biodiesel yield of experimental runs (d) Perturbation plot displaying transesterification variables affecting biodiesel yield from JCO [14].

hexane (2 × 15 mL) simultaneously in order to remove any remnants of organic compound and dried for 5 h at 80 °C in an oven. The obtained result after 7th reaction cycle is now uploaded in excel sheet. No. 6 of the repository data. The reusability of the present catalyst was performed using the optimal reaction parameters. The same transesterification process and recyclability method was performed for 7th reaction cycles and the result of yield is shown in Fig. S4. The graph shows a very minimal drop in yield of biodiesel (97.1 ± 0.4% in 1st cycle to 82.5 ± 0.4% biodiesel yield in 7th cycle). The reduction biodiesel yield was assigned to the loss of catalyst (sulfur content from 1.9 mmol g^{-1} to 1.43 mmol g^{-1}) during the washing process as can be corroborated with SEM-EDX of the recycled catalyst (Fig. S3). FTIR and XRD spectra (Figs. S5 and S6) of the recycled catalyst after 7th reaction cycle showed no distinct dissimilarities with the fresh catalyst, indicating the high stability and aromaticity of the developed carbonaceous GZF-SO_3H catalyst.

Table 2
Design matrix, including experimental variables (A-D) and predicted and actual JCO conversion for the transesterification step [14].

Run no.	Space type	A: MTOR (molar ratio)	B: Catalyst (wt.%)	C: Time (min)	D: Temp. (°C)	Actual biodiesel yield (%)	Prediction biodiesel yield (%)
1	Factorial	30	4	60	80	84.1	83.82
2	Factorial	30	10	40	120	88.1	88.57
3	Center	20	7	50	100	96.5	95.28
4	Center	20	7	50	100	95.6	95.28
5	Factorial	30	4	40	80	75.2	75.64
6	Axial	20	7	70	100	90.1	90.29
7	Factorial	10	4	60	80	66.2	66.02
8	Factorial	10	4	40	80	56.3	56.44
9	Factorial	10	4	40	120	68.1	67.84
10	Axial	20	13	50	100	75.5	75.14
11	Factorial	30	10	40	80	84.2	84.27
12	Factorial	10	10	60	80	74.1	74.31
13	Factorial	10	4	60	120	72.4	72.02
14	Axial	40	7	50	100	85.1	84.91
15	Factorial	10	10	40	120	79.5	79.47
16	Axial	20	1	50	100	60.2	60.57
17	Factorial	30	4	60	120	84.8	85.07
18	Axial	20	7	50	140	87.5	88.01
19	Center	20	7	50	100	94.5	95.28
20	Factorial	30	4	40	120	82.8	82.29
21	Axial	20	7	30	100	83.8	83.62
22	Factorial	30	10	60	120	86.1	85.65
23	Factorial	10	10	60	120	78.1	77.96
24	Factorial	10	10	40	80	70.4	70.42
25	Axial	20	7	50	60	78.2	77.71
26	Axial	10	7	50	100	81.8	82.6
27	Center	20	7	50	100	93.9	95.28
28	Factorial	30	10	60	80	86.2	86.75
29	Center	20	7	50	100	96.3	95.28
30	Center	20	7	50	100	95.5	95.28

4. Experimental Design, Materials and Methods

4.1. Materials

D-(+)-Glucose, $FeCl_3$ and $ZnCl_2$ were supplied from Fisher scientific (99.99% purity). *Jatropha curcas* oil was taken from the local vendor at free of cost from Cachar, Assam, India. Sulphanilic acid (99% purity), H_3PO_2 (99%), Methanol (99.95%) and Ethanol (99%) were procured from Merck. The chemicals were employed as-is without undergoing additional purification. Deionized water was obtained by employing a Simplicity® UV Water Purification System from Merck.

4.2. Methods

The transesterification of *Jatropha curcas* oil to biodiesel was carried out using a conventional approach. In this method, a mixture containing 1 mmol (0.9 g) of *Jatropha curcas* oil, 20 mmol (0.64 g) of methanol, and 8 wt.% (0.072 g) of catalyst relative to the amount of *Jatropha curcas* oil was utilized. The reaction mixture was placed in a 20 mL pressure tube and heated on a magnetic stirrer at 100 °C with a stirring speed of 500 rpm. The reaction proceeded continuously for a duration of 50 min. After that, the catalyst was separated from the reaction mixture through filtration using Whatman 1 filter paper and was subsequently washed multiple times with methanol and hexane. Any excess methanol present in the product was removed using

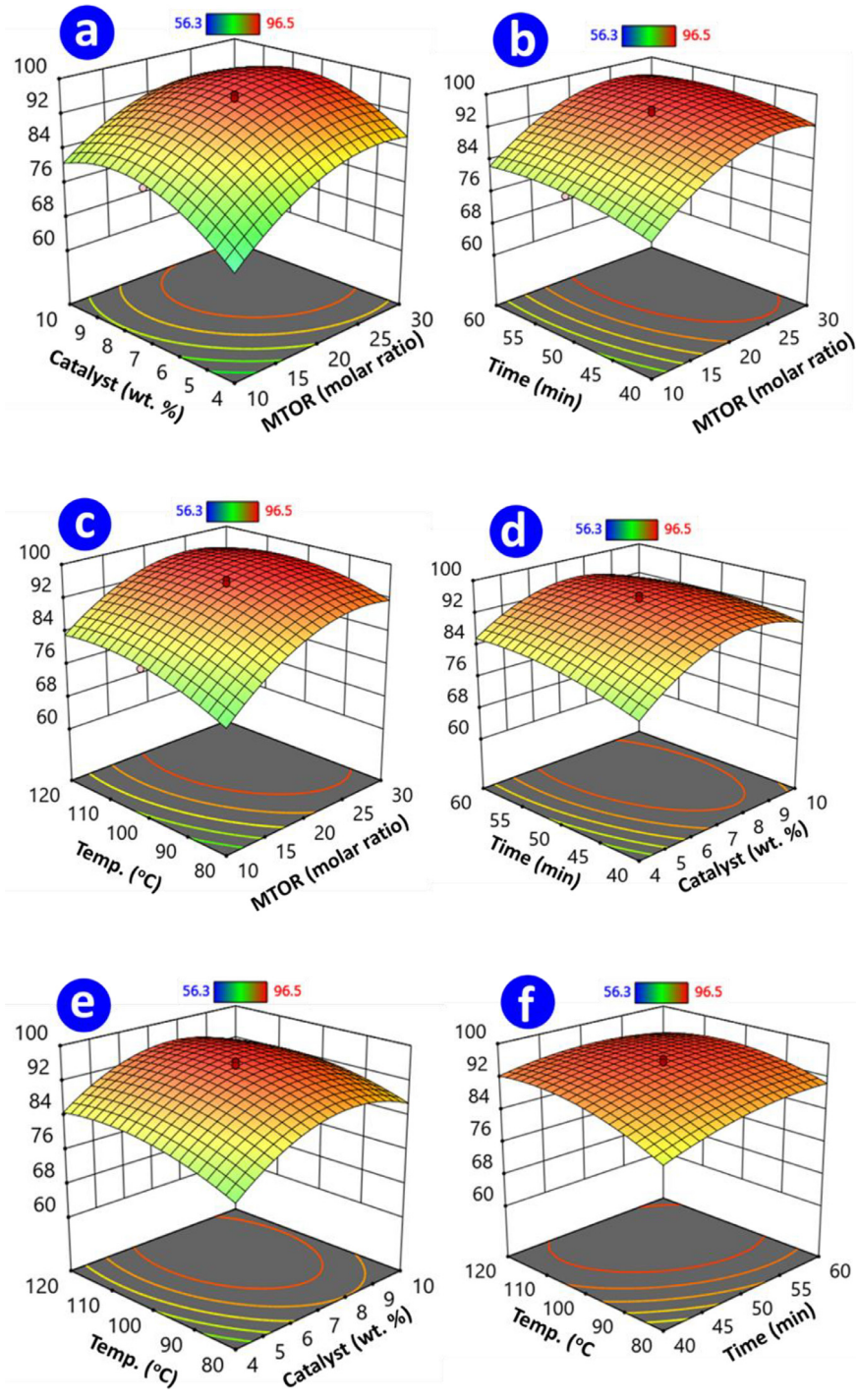

Fig. 7. The efficiency of traditional method biodiesel synthesis from JCO shown in a 3D face diagram for the relation relating the individual variables A-D [14].

Table 3
Statistical result for the regression model of JCO transesterification [14].

Source	Sum of squares	Df	Mean square	F-value	*p*-value	Result	Accuracy test	
							Parameters	Value
Model	3259.04	14	232.79	417.15	< 0.0001	Significant	R^2	0.9974
A- MTOR	848.14	1	848.14	1519.84	< 0.0001		Adjusted R^2	0.9950
B- Catalyst loading	318.28	1	318.28	570.35	< 0.0001		Predicted R^2	0.9927
C- Time	66.67	1	66.67	119.46	< 0.0001		Adequate precision	73.5352
D- Temp.	159.13	1	159.13	285.16	< 0.0001			
AB	28.62	1	28.62	51.29	< 0.0001			
AC	1.96	1	1.96	3.51	0.0805			
AD	22.56	1	22.56	40.43	< 0.0001			
BC	32.49	1	32.49	58.22	< 0.0001			
BD	5.52	1	5.52	9.9	0.0067			
CD	29.16	1	29.16	52.25	< 0.0001			
A^2	580.21	1	580.21	1039.71	< 0.0001			
B^2	1312.65	1	1312.65	2352.22	< 0.0001			
C^2	120.97	1	120.97	216.78	< 0.0001			
D^2	269.45	1	269.45	482.85	< 0.0001			
Residual	8.37	15	0.558					
Lack of fit	3.24	10	0.3242	0.3161	0.9429	Not significant		
Pure error	5.13	5	1.03					
Cor total	3267.41	29						

a rotary evaporator. The resulting product was then analyzed using NMR (Fig. 5) and GC-MS techniques (Table 1) (see ESI for characterization details). For the recycling experiment, the used catalyst was washed with methanol and hexane (two washes of 15 mL each) and dried overnight at 80 °C in an oven. The catalyst was re-weighed before being reused. FTIR comparison graph of biodiesel and JCO feedstock is shown in Fig. S1. The variable used for the FTIR study was attained in the range between 400 and 4000 cm^{-1} with a 3000 Hyperion FTIR spectrometer (Bruker, Germany) at 25 °C. and the data is available in excel sheet no. 3 of the repository data. Furthermore SEM-EDX analysis of catalyst reusability experimental analysis conducted in the laboratory is provided in the supplementary file as Fig. S4 (change in biodiesel yield during catalyst recycle).

4.3. Design of Experiment

RSM was used to investigate the connection involving responses (% yield) and reaction variables A to D (MeOH:JCO molar ratio (A), catalyst loading (B) reaction time (C), temperature (D), and. The RSM-CCD method incorporates a combination of center point and axial point settings to capture non-linear effects in the expected model. The number of experiments (N) required for CCD advancements was determined using the formula $N = 2^n + 2n + m$, where n represents the number of independent variables and m represents the number of replicated central points. In the current study, there were four independent variables ($n = 4$) and six replicated central points ($m = 6$) for the system. Thus, with a total of 30 completed tests (Table 2), the researchers obtained sixteen cube points, eight axial points, and six repeated center data, which were subsequently analyzed in a randomized manner.

The arithmetical implication of the model equation as well as the impact of the variables and their influences on the biodiesel yield were evaluated using analysis of variance (ANOVA). The result of analysis of variance for the biodiesel yield from JCO Table 3. All statistical parameters including analysis of variance (ANOVA) and figures were plotted with the help of Design expert-13 software (Figs. 6 and 7).

Limitations

None.

Ethics Statement

The data presented does not involve any experimentations on humans or animals.

Data availability

Transesterification of Jatropha curcas oil using highly porous sulfonated biochar catalyst: Optimization and characterization dataset (Original data) (Mendeley Data).

CRediT Author Statement

Supongsenla Ao: Investigation, Data curation, Writing – review & editing; **Shiva prasad Gouda:** Data curation; **Manickam Selvaraj:** Writing – review & editing; **Rajender Boddula:** Writing – review & editing; **Noora Al-Qahtani:** Funding acquisition, Writing – review & editing; **Samuel Lalthazuala Rokhum:** Conceptualization, Methodology, Supervision.

Acknowledgements

The authors gratefully acknowledge SAIFs (IITP, IIT Delhi) and CIF NIT SILCHAR for analysis. This work was supported by Qatar University through a National Capacity Building Program Grant (NCBP), [QUCP-CAM-20/23-463]. Statements made herein are solely the responsibility of the authors. Open Access funding provided by the Qatar National Library.

Declaration of Competing Interest

The authors declare that they have no known competing financial interests or personal relationships that could have appeared to influence the work reported in this paper.

Supplementary materials

Supplementary material associated with this article can be found, in the online version, at doi:10.1016/j.dib.2024.110096.

References

[1] S. Kang, J. Ye, Y. Zhang, J. Chang, Preparation of biomass hydrochar derived sulfonated catalysts and their catalytic effects for 5-hydroxymethylfurfural production, RSC Adv. (2013) 7360–7366, doi:10.1039/c3ra23314f.
[2] S. Ao, P.U. Okoye, S. Lalthazuala, W. Ahmad, Sheet-like graphitized glucose-based mesoporous carbon for aqueous adsorption of tetracycline antibiotic, Diam. Relat. Mater. 141 (2024) 110718, doi:10.1016/j.diamond.2023.110718.
[3] T. Kushwaha, S. Ao, K. Ngaosuwan, S. Assabumrungrat, B. Gurunathan, S.L. Rokhum, Esterification of oleic acid to biodiesel using biowaste-based solid acid catalyst under microwave irradiation, Environ. Prog. Sustain. Energy (2023) e14170, doi:10.1002/EP.14170.
[4] R.A. Arancon, H.R. Barros Jr, A.M. Balu, C. Vargas, R. Luque, Valorisation of corncob residues to functionalised porous carbonaceous materials for the simultaneous esterification/transesterification of waste oils, Green Chem. 13 (2011) 3162–3167.

[5] S. Ao, L.A. Alghamdi, T. Kress, M. Selvaraj, G. Halder, A.E.H. Wheatley, S.L. Rokhum, Microwave-assisted Valorization of Glycerol to Solketal using Biomass-Derived Heterogeneous Catalyst, Elsevier, 2023, doi:10.1016/J.FUEL.2023.128190.
[6] Y. Tian, R. Zhang, W. Zhao, S. Wen, Y. Xiang, X. Liu, A new sulfonic acid-functionalized organic polymer catalyst for the synthesis of biomass-derived alkyl levulinates, Catal. Lett. 150 (2020) 3553–3560, doi:10.1007/s10562-020-03253-5.
[7] N.N. Saimon, H.K. Eu, A. Johari, N. Ngadi, M. Jusoh, Z.Y. Zakaria, Production of biodiesel from palm fatty acid distillate by microwave-assisted sulfonated glucose acid catalyst, Sains Malaysiana 47 (2018) 109–115, doi:10.17576/jsm-2018-4701-13.
[8] X.L. Song, X.B. Fu, C.W. Zhang, W.Y. Huang, Y. Zhu, J. Yang, Y.M. Zhang, Preparation of a novel carbon based solid acid catalyst for biodiesel production *via* a sustainable route, Catal. Lett. 142 (2012) 869–874, doi:10.1007/s10562-012-0840-2.
[9] S.L. Rokhum, B. Changmai, T. Kress, A.E.H. Wheatley, A one-pot route to tunable sugar-derived sulfonated carbon catalysts for sustainable production of biodiesel by fatty acid esterification, Renew. Energy 1481 (2021) 01720–01721, doi:10.1016/j.renene.2021.12.001.
[10] L. Sun, C. Tian, M. Li, X. Meng, L. Wang, R. Wang, J. Yin, H. Fu, From coconut shell to porous graphene-like nanosheets for high-power supercapacitors, J. Mater. Chem. A 1 (2013) 6462–6470, doi:10.1039/C3TA10897J.
[11] U.I. Nda-Umar, I. Ramli, E.N. Muhamad, N. Azri, Y.H. Taufiq-Yap, Optimization and characterization of mesoporous sulfonated carbon catalyst and its application in modeling and optimization of acetin production, Molecules 25 (2020) 1–23, doi:10.3390/MOLECULES25225221.
[12] P. Choudhary, A. Sen, A. Kumar, S. Dhingra, C.M. Nagaraja, V. Krishnan, Sulfonic acid functionalized graphitic carbon nitride as solid acid–base bifunctional catalyst for Knoevenagel condensation and multicomponent tandem reactions, Mater. Chem. Front. 5 (2021) 6265–6278, doi:10.1039/D1QM00650A.
[13] L.J. Konwar, P. Mäki-Arvela, E. Salminen, N. Kumar, A.J. Thakur, J.P. Mikkola, D. Deka, Towards carbon efficient biorefining: Multifunctional mesoporous solid acids obtained from biodiesel production wastes for biomass conversion, Appl. Catal. B Environ. 176–177 (2015) 20–35, doi:10.1016/j.apcatb.2015.03.005.
[14] S. Ao, S.P. Gouda, M. Selvaraj, R. Boddula, N. Al-Qahtani, S. Mohan, S.L. Rokhum, Active sites engineered biomass-carbon as a catalyst for biodiesel production: Process optimization using RSM and life cycle assessment, Energy Convers. Manag. 300 (2024) 117956, doi:10.1016/j.enconman.2023.117956.